

New hyperekplexia mutations provide insight into glycine receptor assembly, trafficking and activation mechanisms

Anna Bode*¹, Sian-Elin Wood*², Jonathan G.L. Mullins², Angelo Keramidis¹, Thomas D. Cushion², Rhys H. Thomas^{2,3}, William O. Pickrell^{2,3}, Cheney J.G. Drew^{2,3}, Amira Masri⁴, Elizabeth A. Jones^{5,6}, Grace Vassallo⁷, Alfred P. Born⁸, Fusun Alehan⁹, Sharon Aharoni^{10,11}, Gerald Bannasch¹², Marius Bartsch¹³, Bulent Kara¹⁴, Amanda Krause¹⁵, Elie G. Karam¹⁶, Stephanie Matta¹⁶, Vivek Jain¹⁷, Hanna Mandel¹⁸, Michael Freilinger¹⁹, Gail E. Graham²⁰, Emma Hobson²¹, Sue Chatfield²², Catherine Vincent-Delorme²³, Jubran E. Rahme²⁴, Zaid Afawi²⁵, Samuel F. Berkovic²⁶, Owain W. Howell^{2,3}, Jean-François Vanbellinghen²⁷, Mark I. Rees^{2,3}, Seo-Kyung Chung^{2,3} and Joseph W. Lynch¹

¹The University of Queensland, Queensland Brain Institute and School of Biomedical Sciences, Queensland 4072, Australia. ²Neurology Research and Molecular Neuroscience, Institute of Life Science, College of Medicine, Swansea University SA2 8PP, UK. ³Wales Epilepsy Research Network (WERN), College of Medicine, Swansea University SA2 8PP, UK. ⁴Department of Paediatrics, Division of Child Neurology, Faculty of Medicine, University of Jordan, P.O Box 13002, 11942, Jordan. ⁵Manchester Centre for Genomic Medicine, Central Manchester University Hospitals NHS Foundation Trust, Manchester Academic Health Sciences Centre (MAHSC), Manchester M13 9WL, UK. ⁶Manchester Centre for Genomic Medicine, Institute of Human Development, Faculty of Medical and Human Sciences, University of Manchester, MAHSC, Manchester M13 9WL, UK. ⁷Royal Manchester Children's Hospital, Central Manchester University Hospitals NHS Foundation Trust, Manchester M13 9WL, UK. ⁸Department of Pediatrics, Copenhagen University Hospital, Rigshospitalet, Copenhagen, Denmark. ⁹Department of Pediatrics, Division of Child Neurology, Faculty of Medicine, Başkent University, Ankara, Turkey. ¹⁰Institute of Pediatric Neurology, Schneider Children's Medical Center of Israel, Petah Tikva, Israel. ¹¹Sackler Faculty of Medicine, Tel Aviv University, Tel Aviv, Israel. ¹²Neurology Department, Affinity Medical Group, 1550 Midway Place, Menasha, WI 54952 USA. ¹³Department of Neonatology, University Medical Center of the Johannes Gutenberg University Mainz, Mainz, Germany. ¹⁴Kocaeli University Medical Faculty, Department of Pediatrics, Division of Child Neurology Kocaeli, Turkey. ¹⁵Division of Human Genetics, NHLS and School of Pathology, Faculty of Health Sciences, University of the Witwatersrand, Johannesburg, South Africa. ¹⁶Department of Psychiatry and Clinical Psychology, Saint George Hospital University Medical Center, Balamand University, Faculty of Medicine, Beirut, Lebanon. ¹⁷The Royal Children's Hospital Melbourne, Children's Neuroscience Centre, Royal Children's Hospital, Victoria 3052, Australia. ¹⁸Metabolic Unit, Meyer Children's Hospital, Rambam Medical Center, Technion Faculty of Medicine, Haifa, Israel. ¹⁹Medical University of Vienna, Dept of Pediatrics and Adolescent Medicine, Medical university of Vienna, 1090 Vienna, Austria. ²⁰Department of Genetics, Children's Hospital of Eastern Ontario, Ottawa, Ontario, Canada. ²¹Yorkshire Regional Genetic Service, Chapel Allerton Hospital, Leeds, West Yorkshire, LS9 7TF, UK. ²²Neonatal Unit, Bradford Royal Infirmary, Bradford, West Yorkshire BD9 6RJ, UK. ²³Génétique, Pôle Mère, Enfant, Centre Hospitalier d'Arras, France. ²⁴Clalit Health Services, Shfaram, 20200, Israel. ²⁵Zlotowski Center for Neuroscience, Ben-Gurion University of the Negev, Israel. ²⁶Epilepsy Research Centre, Level 2, Melbourne Brain Centre, 245 Burgundy Street, Austin Health, Heidelberg 3084, Victoria, Australia. ²⁷Institut de Pathologie et de Génétique ASBL / IRSPG, Avenue Georges Lemaître, 25, B-6041 Gosselies, Belgium.

*equal 1st author contribution

Running title: *New glycine receptor hyperekplexia mutations*

To whom correspondence should be addressed: Professor Joseph Lynch, Queensland Brain Institute, University of Queensland, Brisbane, Queensland 4072, Australia. Tel. +617 3346 6375; Fax. +617 3346 6301; Email: j.lynch@uq.edu.au

Keywords: Cys-loop receptor, chloride channel, glycinergic neurotransmission, human startle disease, electrophysiology

Background: Hyperekplexia mutations have provided much information about glycine receptor structure and function.

Results: We identified and characterized nine new mutations. Dominant mutations resulted in spontaneous activation whereas recessive mutations precluded surface expression.

Conclusion: These data provide insight into glycine receptor activation mechanisms and surface expression determinants.

Significance: The results enhance our understanding of hyperekplexia pathology and glycine receptor structure-function.

ABSTRACT

Hyperekplexia is a syndrome of readily provoked startle responses, alongside episodic and generalised hypertonia that presents within the first month of life. Inhibitory glycine receptors are pentameric ligand-gated ion channels (pLGICs) with a definitive and clinically well-stratified linkage to hyperekplexia. Most hyperekplexia cases are caused by mutations in the $\alpha 1$ subunit of the human glycine receptor (hGlyR) gene (*GLRA1*). Here we analysed 68 new unrelated hyperekplexia probands for *GLRA1* mutations and identified 19 mutations of which nine were novel. Electrophysiological analysis demonstrated that the dominant mutations p.Q226E, p.V280M and p.R414H induced spontaneous channel activity indicating this is a recurring mechanism in hGlyR pathophysiology. p.Q226E, at the top of TM1, most likely induced tonic activation via an enhanced electrostatic attraction to p.R271 at the top of TM2, suggesting a structural mechanism for channel activation. Receptors incorporating p.P230S (which is heterozygous with p.R65W) desensitized much faster than wild type receptors, and represents a new TM1 site capable of modulating desensitization. The recessive mutations p.R72C, p.R218W, p.L291P, p.D388A and p.E375X precluded cell surface expression unless co-expressed with $\alpha 1$ wild type subunits. The recessive p.E375X mutation resulted in subunit truncation upstream of the TM4 domain. Surprisingly, on the basis of three independent assays, we were able to infer that p.E375X truncated subunits are incorporated into functional hGlyRs together with unmutated $\alpha 1$ or $\alpha 1$ plus β subunits. These aberrant receptors exhibit significantly reduced glycine sensitivity. To our knowledge, this is the first suggestion that subunits lacking TM4 domains might be incorporated into functional pLGIC receptors.

The glycine receptor chloride channel (GlyR), a member of the pentameric ligand-gated ion channel (pLGIC) family, mediates inhibitory neurotransmission in the spinal cord, brainstem and retina (1). Functional pLGICs comprise of homo- or hetero-pentamers with subunits arranged around a central ion-conducting pore (2). Each subunit contains an extracellular domain (ECD) harbouring the neurotransmitter binding site and a transmembrane domain (TMD) comprising four transmembrane α -helices (TM1-TM4) connected by flexible loops. A total of five GlyR subunit genes exist in humans ($\alpha 1 - \alpha 4$, β), although the $\alpha 4$ (*GLRA4*) locus is considered a pseudo-gene due to a premature stop codon in the TM3-TM4 domain (3). Synaptic GlyRs comprise two α and three β subunits (4,5) although extrasynaptic homomeric α GlyRs are also found (6). Since the $\alpha 1\beta$ GlyR is the sole stoichiometry responsible for inhibitory neurotransmission in motor reflex arcs of the spinal cord (6), mutations impairing the function of either the $\alpha 1$ or β subunit would be expected to impair motor performance.

The evidence for the neuromotor role of the GlyR is provided by the unequivocal link between glycinergic genes and hyperekplexia, a rare neurological disorder (7,8). Hyperekplexia (also known as startle disease) is characterized by readily provoked startle responses, alongside a generalised and episodic hypertonia that presents within the first month of life. A proportion of cases have an increased likelihood of delay in speech acquisition, intellectual disability and recurrent neonatal and infantile apnoeas which gradually normalise during the first years of life. During development into adulthood the condition typically evolves into a life-long predisposition to excessive startle reflexes, triggered by unexpected auditory and tactile stimuli, which then cause startle-induced falls leading to repeated injuries. Hyperekplexia is caused not only by hereditary and *de novo* mutations in the human GlyR $\alpha 1$ and β subunit genes (7,9-13) but also by mutations in other proteins important for the formation and maintenance of glycinergic synapses (14-16). Mutations in the $\alpha 1$ and β subunits result in changes in the surface expression efficiency or in the functional properties of synaptic $\alpha 1\beta$ GlyRs, thereby disrupting inhibitory neurotransmission in motor reflex circuits.

We previously presented the results of a sequencing screen of the GlyR $\alpha 1$ subunit (*GLRA1*) in 88 unrelated hyperekplexia probands from where we identified a total of 19 mutations, twelve of which were novel (10). We demonstrated that dominant mutations typically disrupt receptor function without changing their surface expression

efficiency whereas recessive mutations generally preclude functional receptor expression when expressed either as mutated $\alpha 1$ homomers or as heteromers with the β subunit. In the present study, 68 new unrelated patients with a clinical diagnosis of hyperekplexia were screened for mutations in *GLRA1*. The screening revealed a total of 19 mutations of which nine were novel. All new mutations were characterized in terms of their electrophysiological properties and their cell surface localization. Additionally, a previously characterized mutation, p.R65W (10), was re-investigated due to its presumed compound heterozygosity with the new mutation, p.P230S. The subsequent functional investigation of the hyperekplexia mutations revealed three residues critical for GlyR channel opening, providing insight into pLGIC activation mechanisms, and one novel residue playing an important role in desensitization.

EXPERIMENTAL PROCEDURES

Patient samples - A total of 68 unrelated probands with a clinical diagnosis of hyperekplexia were recruited for this study with appropriate ethical approval and consent procedures in place (South West Wales REC). Referral was initiated from neurologists, paediatricians, or clinical geneticists from the UK and several international centres. Diagnostic criteria for hyperekplexia included a non-habituating startle response (positive nose tap test), often with neonatal apnoea, a history of infantile hypertonicity, and clinical exclusion of phenocopies such as startle epilepsy or early encephalopathy (17,18).

Molecular genetics - Multiplex PCR amplification (Qiagen, UK) was employed to rapidly amplify all coding exons and flanking intronic regions of *GLRA1*. Purified PCR amplicons were Sanger sequenced using ABITM capillary technology (Foster City, USA). The frequency of variants identified was determined by screening a panel of 100 commercial control samples using restriction fragment length polymorphism (RFLP) if a suitable restriction enzyme was available, or by high-resolution melt analysis performed on LightScanner (Idaho Technologies, USA). Detection of large deletions or insertions was performed using Multiplex Ligation-Dependent Probe Amplification (MLPA, MRC-Holland) according to the manufacturer's protocol. Additionally, confirmation of the recurrent exon 1-7 deletion mutation was carried out using a breakpoint PCR analysis (19). Mutations were introduced into pRK5-hGlyR $\alpha 1$ using the QuikChange site-directed mutagenesis kit (Stratagene, UK) and

confirmed by direct sequencing of the entire transgene-coding region (10).

Fluorescence-based imaging - Experiments were performed on HEK AD293 cells cultured in Dulbecco's modified Eagle's medium supplemented with 10% fetal calf serum and 1% penicillin/streptomycin. The $\alpha 1$ wild type subunit, the β wild type subunit and the plasmids containing hyperekplexia mutations were all co-transfected in equal amounts. The pcDNA3-YFP-I152L plasmid was co-transfected in an amount equal to the sum of all transfected GlyR plasmid amounts. When the transfection was terminated 16 h later by rinsing with fresh culture medium, cells were plated into the wells of a 384-well plate. Within the following 24 – 32 h, the cell culture medium was replaced by an extracellular control solution (140 mM NaCl, 5 mM KCl, 2 mM CaCl₂, 1 mM MgCl₂, 10 mM HEPES, and 10 mM glucose, pH 7.4). Cells were imaged with an automated fluorescence-based screening system using YFP-I152L fluorescence quench as an indicator of anion influx rate (20). During experiments, fluorescence images of each well were obtained twice: once before and once after the application of a sodium iodide solution (140 mM NaI, 5 mM KCl, 2 mM CaCl₂, 1 mM MgCl₂, 10 mM HEPES, and 10 mM glucose, pH 7.4) containing defined concentrations of glycine. Mean percentage quench values represent data averaged from four experiments carried out on different plates. Each experimental value was an average of the percentage quench of all fluorescent cells in three wells on the same plate, with each well containing > 200 cells. To determine the glycine dose-response curve from these data, an empirical three parameter Hill equation was fitted by a non-linear least squares algorithm using SigmaPlot 12.0 software.

Electrophysiology - Glycine-gated currents were measured in HEK AD293 cells transfected as described above. Recordings were performed by whole-cell patch-clamp electrophysiology at a holding potential of -40 mV. Alternatively, spontaneous single-channel currents were recorded from outside-out excised patches, held at -70 mV in the absence of agonist, except for $\alpha 1$ wild type receptors, which opened too infrequently in glycine-free solution to obtain accurate estimates of current amplitude. Current amplitude for wild type receptors was instead estimated from recordings in the presence of 1 mM glycine. During experiments, cells were continually superfused with the extracellular control solution as detailed above. Patch pipettes were pulled to a final tip resistance of 1 – 4 M Ω (whole-cell) or 6 – 12 M Ω (outside-out) when filled with a standard intracellular solution (145 mM CsCl, 2 mM CaCl₂, 2 mM

MgCl₂, 10 mM HEPES, and 10 mM EGTA, pH 7.4). Whole-cell currents, which were filtered at 1 kHz and digitized at 2 kHz, were recorded using an Axon MultiClamp 700B amplifier (Molecular Devices). Single-channel currents, filtered at 5 kHz and digitized at 20 kHz, were recorded using an Axon Axopatch 200B amplifier (Molecular Devices). Voltage-clamp fluorometry experiments were performed as previously described (21). Briefly, oocytes were removed from the ovaries of *Xenopus laevis* frogs, incubated in OR-2 (82.5 mM NaCl, 2 mM KCl, 1 mM MgCl₂, and 5 mM HEPES, pH 7.4) containing 1.5 mg/ml collagenase for 2 h at room temperature on a shaker and co-injected with 5 ng pGEMHE-hGlyR α 1 and 25 ng pGEMHE-hGlyR α 1-R271C/E375X RNA into the cytosol. Oocytes were cultured for 2 – 3 days at 18 °C in ND96 (96 mM NaCl, 2 mM KCl, 1 mM MgCl₂, 1.8 mM CaCl₂, and 5 mM HEPES, pH 7.4) containing 275 mg/l sodium pyruvate, 110 mg/l theophylline and 0.1 % (v/v) gentamicin. For labelling, oocytes were incubated with 10 μ M sulforhodamine methanethiosulfonate (MTSR) diluted in ND96 for 1 min on ice. 3 mM KCl was used as internal solution and recordings were performed at -40 mV.

Immunofluorescence - GlyR α 1 subunits were transiently expressed in HEK293 cells using the MagnetofectionTM method (Oz Biosciences). Around 24 h post-transfection, cells were fixed in 4 % (w/v) paraformaldehyde (PFA) for 5 min at room temperature. Cells were quenched with 50 mM NH₄Cl in PBS. Fixed cells were permeabilised with PBS containing 0.1 % (v/v) Triton X-100 (Sigma), 10 % (v/v) fetal calf serum (Sigma) and 0.5 % (w/v) bovine serum albumin (fraction V; Sigma) to allow for intracellular immunostaining. Receptor sublocalization was determined using rabbit monoclonal anti-GlyR α 1 (1:400, Millipore) primary antibody and with goat anti-rabbit secondary antibody, conjugated with AlexaFluor 488 (1:200, Invitrogen). Cell surface immunostaining was conducted using the same reagents, antibodies and dilutions but carried out prior to PFA fixation. Fixed cells were then quenched with 50 mM NH₄Cl before mounting on glass slides. Cell images were acquired using a Zeiss LSM 710 confocal microscope with ZEN software. The master gain was kept constant to compare the expression of α 1 GlyR mutants relative to wild type. Transfection was repeated three times.

Molecular modelling - Wild type and mutated forms of the human α 1 GlyR were modelled by 50 % homology (69 % sequence coverage) with PDB structure 3RHW, the glutamate-gated chloride channel receptor (α GluClR) from *C. elegans* (22).

Using our multi-template homology modelling pipeline, this was one of three PDB homologues that were identified and used in the assembly of the α 1 GlyR models, 3RHW (chain E), 1VRY (chain A) and 1MOT (chain A). The homology modelling pipeline was built with the Biskit structural bioinformatics platform (23). Our pipeline workflow incorporates the NCBI tools platform (24), including the BLAST program for similarity searching of sequence databases. T-COFFEE (25) was used for alignment of the test sequence with the template, followed by iterations of the MODELLER-9.11 program (26) to generate the final model structure. The Chimera program (27) was used for the viewing of models and generation of images.

RESULTS

Mutation analysis - A total of 68 probands with hyperekplexia were assessed for genetic variation in *GLRA1* coding regions. All sequence variations were cross-referenced with the dbSNP database and our previous *GLRA1* datasets (for recurrent mutations) and were regarded as probable mutations following exclusion from a panel of 100 control samples and exome variants server (<http://evs.gs.washington.edu/EVS/>). The screening revealed 19 mutations in 21 hyperekplexia probands (Table 1), a rate which is consistent with previous studies (10,28). Nine mutations were novel in the public domain and three (one novel and two recurrent) mutations were present in more than one individual. Note that p.R414H has since been reported as a very rare variant in dbSNP (rs200130685), with a heterozygosity of 0.002 and a Minor Allele Frequency (MAF) of 0.0233 from the exome variants server. Consistent with previous studies, deletion and nonsense mutations were associated with recessive inheritance (homozygous or compound heterozygous) whereas missense mutations resulted in a dominant or recessive effect depending on their position in the polypeptide. The majority of index cases showed recessive inheritance (15 / 21; 71 %) including cases 12 and 19 with confirmed compound heterozygosity as mutations were segregated back to parental DNA. It is likely that sample 5 represents a third case of compound heterozygosity; however, parental DNA was not available for confirmation. Four index cases of Turkish origin displayed a recessive homozygous deletion of exons 1-7 further confirming this deletion as a significant population-specific risk-allele (10,29). Dominant mutations were mainly located in the discrete transmembrane α -helices whereas recessive mutations were spread throughout the protein. Phylogenetic alignment of

all novel missense mutations established that they altered conserved amino acids and were protein-damaging when assessed using Sorting Intolerant from Tolerant (SIFT) tool (accessible at <http://sift.jcvi.org/>). The functional impact of the novel mutations was further investigated under recombinant conditions that simulated the dominant, recessive and compound heterozygous inheritance modes.

Functional high-throughput analysis - The first round of functional characterization involved imaging live transfected cells via an automated fluorescence-based screening system using YFP-I152L fluorescence quench as an indicator of anion influx rate (20). The advantage of this approach over electrophysiology is that responses of large cell numbers can be averaged, thus permitting the reliable quantitation of small changes in the functional expression levels of mutated GlyR isoforms. To investigate the functional properties of the mutated receptors, HEK AD293 cells were transiently transfected with wild type and mutated subunits in various combinations in an attempt to simulate dominant, recessive and compound heterozygous inheritance modes. Each mutated subunit was expressed on its own, with the β wild type subunit, with the $\alpha 1$ wild type subunit and with both $\alpha 1$ and β wild type subunits together. These experiments are summarized as: 1) mutant alone, 2) mutant + β , 3) mutant + $\alpha 1$, 4) mutant + $\alpha 1\beta$. For compound heterozygous mutations, the mutated subunits were also co-transfected together with and without the β wild type subunit, i.e., 5) 1st mutant + 2nd mutant, 6) 1st mutant + 2nd mutant + β . Fluorescent cells were considered as expressing functional GlyRs when the quench was a least 10 % greater than the quench from cells expressing YFP only (no receptors).

Glycine dose-response experiments showed that the glycine sensitivity was reduced for all recessive and compound heterozygous mutations relative to $\alpha 1$ wild type GlyRs (Fig. 1A). With the exception of the p.P230S mutation which expressed as a homomer, the recessive and compound heterozygous mutated subunits only showed a response to glycine if the $\alpha 1$ wild type subunit was co-expressed. Note that co-expression of these mutated $\alpha 1$ subunits with the β wild type subunit did not produce functional expression. Receptors incorporating both compound heterozygous mutations, p.L291P and p.D388A, showed no evidence of glycine sensitivity regardless of the presence of the β subunit. In contrast, receptors incorporating both p.R65W and p.P230S responded to glycine with and without β subunit co-expression, albeit with dramatically reduced

glycine sensitivity. As the glycine sensitivity was decreased for all mutated subunits when co-expressed with the $\alpha 1$ wild type subunit, we concluded that all recessive and compound heterozygous mutated subunits were incorporated into functional GlyRs as heteromers, if not as homomers.

For the three novel dominant mutations, in the case of p.R414H, no significant change in glycine EC₅₀ was detected (Fig. 1A), and for receptors containing the dominant mutations p.Q226E and p.V280M, the glycine sensitivity could not be determined as fluorescence quench was complete in the absence of glycine. To test whether these three mutations formed spontaneously active channels, we initially bathed cells in NaCl solution and then introduced a high concentration of NaI solution containing no glycine. The results of this experiment, summarised in Fig. 1B, show that receptors containing p.Q226E, p.V280M or p.R414H subunits displayed significant quench in the absence of glycine. As iodide is highly permeant through GlyRs and quenches YFP-I152L fluorescence much more potently than chloride does, this result provides evidence that these three mutations result in spontaneously active or 'leaky' channels. Indeed, the high level of spontaneous activity was the reason why the glycine sensitivity of receptors incorporating p.Q226E and p.V280M mutations could not be quantitated (Fig. 1A).

In addition, for all functional channels, the anion influx rate was significantly reduced relative to $\alpha 1$ wild type receptors as indicated by their reduced maximal glycine-induced fluorescence quench magnitude (Fig. 1C). As noted above, the fluorescence quench for p.Q226E- and p.V280M-containing GlyRs was already maximal in the absence of glycine. Moreover, the percentage of quenched cells relative to the total number of fluorescent cells was significantly reduced for all functional channels relative to $\alpha 1$ wild type receptors (except for p.R414H) suggesting that fewer functional receptors are located at the cell surface (Fig. 1D). This observation suggests that the mutations tend to impair functional receptor expression.

Spontaneous activity as a mechanism for dominant hyperekplexia mutations - We then employed patch-clamp electrophysiology to analyse the effects of the mutations on receptor function at greater precision. Examples of currents activated by increasing glycine concentrations at homomeric $\alpha 1$ GlyRs together with the averaged glycine dose-response relationship are shown in Fig. 2. The mean glycine EC₅₀ value of p.Q226E indicates that the glycine sensitivity was not significantly altered

(Fig. 2A, Table 2). In contrast, for receptors incorporating the dominant mutation p.V280M, the sensitivity to glycine was dramatically increased relative to wild type receptors (Fig. 2B, Table 2). The mean glycine EC₅₀ value of p.R414H was modestly increased (Fig. 2C; Table 2). These results are broadly consistent with the fluorescence data shown in Fig. 1.

For the three novel dominant mutations, our fluorescence assay predicted spontaneous activity for p.Q226E, p.V280M and p.R414H receptors (Fig. 1B) which was then further investigated by recording single channel activity in outside-out membrane patches bathed in glycine-free extracellular solution. Recordings revealed spontaneous activity for all three mutated homomeric receptors whereas little, if any, spontaneous activity was ever observed for wild type $\alpha 1$ GlyRs (Fig. 3A) consistent with previous reports (30). At a membrane potential of -80 mV, the single channel current amplitude for p.Q226E receptors was smaller (4.5 ± 0.1 pA, $n = 4$ patches, Fig. 3B) than for wild type $\alpha 1$ receptors (7.2 ± 0.1 pA, $n = 3$, Fig. 3A), whereas the amplitude for p.V280M receptors was unchanged (7.1 ± 0.2 pA, $n = 3$, Fig. 3C) and the magnitude of p.R414H receptors was larger (8.4 ± 0.2 pA, $n = 3$, Fig. 3D). The corresponding conductance values at -70 mV, a Cl⁻ equilibrium potential of 0 mV, and a liquid junction potential of 4 mV, were; 97.3 pS, 60.8 pS, 95.9 pS and 110.8 pS for wild type, p.Q226E, p.V280M and p.R414H receptors, respectively. Applying a saturating concentration of glycine, measuring the peak current response and dividing that by the single channel amplitude provided an estimate of the minimum number of channels contained in each recorded patch. Open probability (Po) was determined using segments of record that contained no evidence of multiple, superimposed openings. A total of 5 - 6 minutes of recording was selected across 3 - 4 patches for each channel type. Estimated Po values determined in this way should be regarded as upper limits and were as follows: p.Q226E, 0.03; p.V280M, 0.07; p.R414H, <0.001. Wild type homomeric receptors opened too infrequently in glycine-free solution to obtain a reliable Po measurement. It was, however, dramatically reduced relative to the mutated GlyRs.

Incorporation of TM4 truncated subunits - Subunits incorporating the recessive mutations, p.R72C, p.R218W or p.E375X, were only functional when co-expressed with the $\alpha 1$ wild type subunit. The glycine sensitivities and the maximal current amplitudes of receptors incorporating these mutations were reduced relative to those of wild type receptors (Fig. 4A-D, Table 2) in agreement

with the results from the fluorescence assay (Fig. 1). For all $\alpha 1\beta$ heteromeric receptors, β subunit incorporation was confirmed pharmacologically by its characteristic reduction in sensitivity to lindane inhibition (31). For example, in Fig. 4D (lower panel) we confirmed that $\alpha 1$ wild type GlyRs are strongly inhibited by 100 μ M lindane, whereas $\alpha 1\beta$ wild type GlyRs are resistant. As receptors formed by co-expression of p.E375X, $\alpha 1$ wild type and β wild type subunits were also resistant to lindane and showed decreased glycine sensitivity relative to $\alpha 1\beta$ GlyRs (Fig. 4D, Table 2), we infer that p.E375X subunits were incorporated into functional $\alpha 1\beta$ heteromeric GlyRs.

We were surprised to observe that the truncation mutation, p.E375X, which has lost the TM4 domain, reduced the glycine sensitivity significantly ($p < 0.001$ relative to $\alpha 1$ wild type via unpaired t-test) when co-expressed with the $\alpha 1$ wild type subunit (Fig. 4C, D). The reduced glycine sensitivity was only partly compensated by co-expressing the β wild type subunit. This result strongly suggests that the truncated subunit is incorporated into functional receptors which is unexpected given that previous GlyR studies indicated that TM4 deletion is incompatible with the surface expression of functional $\alpha 1$ GlyRs (32-35). Given our unexpected result, we sought to confirm whether the p.E375X mutant subunit was incorporated into functional GlyRs using voltage-clamp fluorometry.

Voltage-clamp fluorometry involves introducing a cysteine into a receptor domain of interest and covalently tagging it with a sulfhydryl-labelled fluorophore, commonly a rhodamine derivative such as MTSR. Because the quantum efficiency of rhodamine fluorescence is proportional to the hydrophobicity of its environment, a glycine-induced fluorescence change can be interpreted as a local conformational change at the labelled site (36). Voltage-clamp fluorometry is thus able to report conformational rearrangements in real time at defined locations on the surface of the labelled subunit. These experiments were performed on receptors expressed in *Xenopus* oocytes as HEK293 cells exhibit an unacceptably high level of non-specific MTSR labelling. The MTSR-labelled p.R271C mutant $\alpha 1$ GlyR produces a fluorescence change of ~20 % upon activation with 10 mM (saturating) glycine (21). When the p.E375X truncation subunit, also labelled at p.R271C, was expressed together with the $\alpha 1$ wild type subunit, the activation of the recombinant receptors by saturating (10 mM) glycine generated currents with a mean maximal current amplitude of 4.8 ± 0.5 μ A and a maximal change in fluorescence of 0.7 ± 0.1

% (n = 4; Fig. 4E). Control current and fluorescence traces from an MTSR-labelled p.R271C mutant GlyR are also shown. In contrast, unlabelled GlyRs comprising the same subunits yielded no significant glycine-induced fluorescence change (data not shown). This provides strong evidence for the surface expression of p.E375X subunits, and also suggests they experience a conformational change upon glycine-induced receptor activation. As the fluorescence change we observed is smaller than the change in fluorescence for homomeric p.R271C mutant $\alpha 1$ GlyRs (21), we infer that the p.E375X subunit is either incorporated into functional receptors at a low rate or that its conformational change is different from that of full length p.R271C $\alpha 1$ GlyRs.

Functional effects in heterozygous state - Receptors incorporating the compound heterozygous mutation p.R65W showed drastically decreased glycine sensitivity and decreased maximal current amplitudes independent of β subunit expression (Fig. 5A; Table 2). The p.P230S mutation also decreased glycine sensitivity and maximal current amplitudes in the presence and absence of the β subunit (Fig. 5B; Table 2). All electrophysiological results for the p.R65W and p.P230S mutations are consistent with the fluorescence data described above (Fig. 1). It is also evident in Fig. 5B that p.P230S induces fast desensitization. These receptors exhibited a mean decay time constant of 0.9 ± 0.3 s for 3 mM glycine (*c.f.*, wild type receptors: 7.2 ± 1.7 s). Receptors containing the compound heterozygous mutations p.L291P or p.D388A were only functional when each mutated $\alpha 1$ subunit was co-expressed with the $\alpha 1$ wild type subunit (Fig. 1). Electrophysiological recordings revealed that the p.L291P mutation decreased glycine sensitivity but not maximal current amplitudes (Fig. 5C; Table 2). The p.D388A mutation decreased glycine sensitivity and maximal current amplitudes (Fig. 5D; Table 2). For both mutations, the changes relative to wild type receptors were independent of β subunit expression. Again, these results are consistent with the fluorescence data presented in Fig. 1.

Cell surface localization - Confocal microscopy of transfected cells immunostained with an $\alpha 1$ GlyR antibody was performed to analyse subcellular localization of wild type and mutated receptors. Permeabilised cells were used to determine the intracellular sublocalization of receptors with all constructs showing comparable intracellular expression (Fig. 6, left hand image of each image pair). Cell surface expression was visualised in non-permeabilised cells. Cells transfected with

wild type and the dominant mutations p.V280M and p.R414H showed immunoreactivity around the cellular circumference indicating localization at the surface (Fig. 6, right images), suggesting these variants do not affect integration of GlyRs into the cell membrane. The p.Q226E dominant mutation showed reduced immunoreactivity at the cell surface, suggesting it may impair integration into the surface membrane, unlike the other dominant mutations. The cell surface expression levels of recessive mutated receptors observed in this study showed partial or complete loss of cell surface accumulation. The recessive mutations p.R65W, p.P230S and p.L291P showed decreased integration into the surface membrane with only partial punctate staining, whilst p.R72C, p.R218W, p.D388A and p.E375X were completely absent from the cell membrane displaying only cytoplasmic staining (Fig. 6, right images). Surface accumulation of $\alpha 1$ subunits containing these mutations was not detectable with any of the three transfection procedures.

Molecular modelling - A homology model based on the *C. elegans* α GluClR crystal structure was used to determine structural mechanisms by which novel mutations disrupted GlyR structure and function (Fig. 7). In particular, the spontaneously active channel p.Q226E affected the TM1 domain towards its extracellular end (Fig. 7A, B). Structural modelling showed extension of the TM2 and TM3 helices at their extracellular end, along with extension of the TM4 helix at its intracellular end. Given that p.Q226E faces across the subunit interface towards p.R271 of the adjacent subunit (not shown), an enhanced electrostatic attraction between these two residues may be responsible for the tonic activity induced by p.Q226E. The other spontaneous opener p.V280M affected the extracellular loop between the TM2 and TM3 domain (Fig. 7C). This mutation was also found to introduce a kink at the extracellular end of the TM1 helix, perhaps via an altered energetic or steric interaction with I225 across the subunit interface. Also, the TM2 helix was extended at its extracellular end whereas the TM4 helix was extended at its intracellular end, along with a conformational change at this site. We also observed changes to the conformation of the extracellular domain. In the p.V280M receptor, the α -helix that is found in the wild type subunit between D12 and R20 was lost and a short helix was introduced around position 72 which would explain its dramatically altered glycine sensitivity. p.R414H affected the C-terminal region at the extracellular end of the TM4 domain causing profound loss of helical conformation at the

cytoplasmic end of the TM4 domain and extension of the TM2 helix at its extracellular end (Fig. 7D). Structural modelling suggested that the truncation mutation p.E375X, which lacks the TM4 domain, caused major conformational changes in the TM2 helix via extension of the TM2 helix at its extracellular end and loss of the short helix at the top of the extracellular domain (Fig. 7E). The fast desensitizer p.P230S affected the TM1 domain, directly causing a major conformational change by introducing a profound kink at the extracellular end (Fig. 7F). In addition, a major conformational change at the cytoplasmic end of the TM3 helix was detected, producing another kink, and substantial changes to the TM4 helix. Conformational changes in the extracellular domain included loss of the short helix at the top and β sheet compression.

The impact of the novel dominant mutations upon the pore radius is shown in Fig. 7G. For the spontaneously active receptors p.Q226E and p.V280M, a channel widening of 1.3 Å and 4.3 Å, respectively, at the cytoplasmic exit was detected relative to wild type receptors which is consistent with the observations of a leaky channel. In contrast, the mutation p.R414H had no effect on the pore diameter at the cytoplasmic exit but demonstrates substantial widening towards the extracellular entry explaining the observed spontaneous channel openings.

DISCUSSION

This study has identified a further 21 *GLRA1*-positive hyperekplexia probands (Table 1) with 19 mutations, of which nine were novel, adding to the compendium of *GLRA1* mutations. Consistent with previous studies (10,37-40), dominant mutations were expressed at the cell surface thereby causing changes to the glycine sensitivity, conductance and/or open probability. In contrast, recessive and compound heterozygous mutations mainly affected cell surface trafficking and insertion of receptors into the membrane (10,41-43). The mechanisms by which each novel mutation caused hyperekplexia will now be considered in detail.

Genetic screening identified three novel autosomal dominant mutations, p.Q226E, p.V280M and p.R414H, that each produced spontaneously active channels. Prior to this study, only one hyperekplexia mutation (Y128C) was known to produce spontaneous activity (10). This mutation was also autosomal dominant. Spontaneous activity was evident not only in mutated homomeric channels, but also in channels formed by the co-expression of mutated subunits and $\alpha 1$ wild type subunits and/or β wild type

subunits (Fig. 1, 2). Structural modelling predicted that the mutations p.Q226E and p.V280M cause a widening of the outer channel pore leading to spontaneous activity. The p.V280M mutation dramatically increased both the level of spontaneous activity and glycine sensitivity, suggesting a drastic destabilisation of the closed channel state. The loss of the β sheet structure around the constraining loop C glycine binding domain is likely to impact upon glycine binding and retention, rendering the glycine binding site much more accessible. The kink introduced by p.V280M to the cytoplasmic end of the TM3 domain affects the close TM2-TM3 packing, reducing the stability of the closed channel, due to greater conformational freedom at the cytoplasmic end of the TM2 domain. Given that p.V280M-containing GlyRs expressed strongly at the cell surface (Fig. 6), the high level of spontaneous activity may partly explain the observed reduction in peak glycine-induced current magnitude. A reduction in the glycine-inducible current magnitude, coupled with a possible diminution of the chloride electrochemical gradient caused by the high level of spontaneous activity, may be among the mechanisms by which the p.V280M mutation disrupts glycinergic signalling.

In contrast, the glycine sensitivities of p.Q226E- and p.R414H- containing receptors were similar to that of wild type receptors and both mutations caused spontaneous activity. However, modest reductions in the single channel conductance and the cell surface expression efficiency would have reduced the chloride flux-carrying capacity of p.Q226E-containing GlyRs and therefore may have contributed to the hyperekplexia phenotype (Fig. 2D, 6). Given that p.Q226E is closely apposed with p.R271 of the adjacent subunit, we hypothesise that the enhanced electrostatic attraction between these oppositely-charged residues may be responsible for the tonic receptor activity. In the p.R414H GlyR, the extremely low spontaneous open probability seems unlikely to have caused a hyperekplexia phenotype on its own, as the expression efficiency and glycine sensitivity were not diminished relative to that of wild type receptors. One possibility is that the mutation altered TM4 orientation and thus TM3-TM4 loop structure, leading to a change in propensity of this subunit to bind clustering proteins at synapses. No effect on the predicted structure of the extracellular domain fits with wild type comparable glycine sensitivity seen for this mutation. However, the main difference to the wild type monomer is the loss of α -helical structure at the cytoplasmic end of the TM4 domain. This region is at the outside of the pentamer and contains an unusually high proportion of charged

residues for a transmembrane region, 382-QRAKKIDKISR-392, which is completely disrupted in p.R414H receptors.

The recessive p.R72C, p.R218W and p.E375X mutations all precluded the surface expression of mutated homomeric GlyRs (Fig. 1, 4). However, when each mutated subunit was co-expressed with $\alpha 1$ wild type or $\alpha 1$ and β wild type subunits, robust glycine-activated currents were observed. As the glycine sensitivity of the resultant p.E375X receptor was significantly decreased relative to homomeric $\alpha 1$ GlyRs, we infer that the p.E375X subunit was incorporated into functional receptors together with either $\alpha 1$ subunits alone or with $\alpha 1$ plus β subunits. Because this result was unexpected, it was substantiated using voltage-clamp fluorometry (Fig. 4E). We also attempted to confirm it using immunofluorescence, but the incorporation rate may have been too low to allow surface expression to be detected. As noted above, we were surprised that the p.E375X subunit was incorporated given that previous studies have shown that TM4 deletion is incompatible with the surface expression of functional $\alpha 1$ GlyRs (32-35). Indeed, the deletion of only a few residues at the C-terminal end of the TM4 domain is sufficient to render some pLGIC receptors completely non-functional (12,44,45).

To our knowledge, this is the first suggestion that a pLGIC receptor subunit may be functionally expressed without a TM4 domain. The human GlyR $\alpha 4$ subunit (Uniprot accession number Q5JXX5) has long been regarded as a pseudo-gene because it incorporates a stop codon that truncates the receptor prior to the TM4 domain (Simon et al., 2004). The truncation occurs at the D383 residue which corresponds to Q382 in the $\alpha 1$ subunit. As this is C-terminal of E375, it is possible that the $\alpha 4$ subunit may be incorporated into functional GlyRs suggesting it could exert a physiological role in modulating the functional properties of GlyRs. There may also be a case to reassess the pathophysiology of the other pLGIC late protein truncating events in epilepsy and related disorders, for example GABA type-A receptor mutations (46).

Genetic analysis suggested possible heterozygosity between p.R65W and p.P230S although parental DNA was not available to confirm this. We previously described p.R65W as recessive on the basis of both the genetic analysis and a trafficking defect when expressed in the homozygous state (10). The present study shows that GlyRs comprised of p.R65W plus $\alpha 1$ and β wild type subunits exhibited a 20-fold increase in

the glycine EC₅₀ value (Fig. 1, 5). As this reduction in glycine sensitivity should be easily enough to cause hyperekplexia on its own (47,48), it implies that the p.R65W mutation should be inherited in an autosomal dominant manner. It therefore remains a mystery why heterozygous parents remain asymptomatic, possibly implying the existence of compensating physiological mechanisms. The p.P230S mutation produced fast desensitising receptors, reduced peak glycine-activated current magnitude and modestly reduced glycine sensitivity (Fig. 1, 5). All of these effects remained when the mutated subunit was co-expressed with $\alpha 1$ and/or β wild type subunits, implying that p.P230S should also exhibit an autosomal dominant inheritance mode. As expected, when p.R65W, p.P230S and β wild type subunits were co-expressed to mimic compound heterozygosity, glycine sensitivity and peak current magnitudes were drastically reduced (Fig. 1A, C), readily accounting for the hyperekplexia phenotype.

As R65 forms a crucial component of the glycine binding site (5,49), the non-conservative p.R65W mutation most likely disrupts glycine binding when functionally expressed with wild type subunits. Our finding that it is not trafficked to the surface when expressed as a homomer (Fig. 1) is most likely the result of a global structural disruption caused by this mutation (10). As GlyR desensitization involves a specific conformational change at the ECD-TMD interface (50), the effect of the p.P230S mutation on desensitization may be due to a conformational change at this interface.

Genetic analysis confirmed that the p.L291P and p.D388A mutations exhibited compound heterozygosity. Our functional analyses revealed that both mutated subunits did not express as homomers and exhibited reduced glycine sensitivity when individually co-expressed as heteromers with $\alpha 1$ and β wild type subunits (Fig. 1, 5). We were unable to detect functional surface expression following co-expression of both p.L291P and p.D388A with β wild type subunits which would account for the hyperekplexia phenotype.

In conclusion, this study illustrates the importance of hyperekplexia mutations in identifying new insights into the structure and function of GlyRs and other pLGIC family members. This in turn allows us to provide a more definitive explanation of the phenotype and clinical impact of the gene-positive patients through stratification of disease mechanisms.

REFERENCES

1. Lynch, J. W. (2004) Molecular structure and function of the glycine receptor chloride channel. *Physiol Rev* **84**, 1051-1095
2. Corringer, P. J., Baaden, M., Bocquet, N., Delarue, M., Dufresne, V., Nury, H., Prevost, M., and Van Renterghem, C. (2010) Atomic structure and dynamics of pentameric ligand-gated ion channels: new insight from bacterial homologues. *J Physiol* **588**, 565-572
3. Simon, J., Wakimoto, H., Fujita, N., Lalande, M., and Barnard, E. A. (2004) Analysis of the set of GABA(A) receptor genes in the human genome. *J Biol Chem* **279**, 41422-41435
4. Yang, Z., Taran, E., Webb, T. I., and Lynch, J. W. (2012) Stoichiometry and subunit arrangement of alpha1beta glycine receptors as determined by atomic force microscopy. *Biochemistry* **51**, 5229-5231
5. Grudzinska, J., Schemm, R., Haeger, S., Nicke, A., Schmalzing, G., Betz, H., and Laube, B. (2005) The beta subunit determines the ligand binding properties of synaptic glycine receptors. *Neuron* **45**, 727-739
6. Lynch, J. W. (2009) Native glycine receptor subtypes and their physiological roles. *Neuropharmacology* **56**, 303-309
7. Bakker, M. J., van Dijk, J. G., van den Maagdenberg, A. M., and Tijssen, M. A. (2006) Startle syndromes. *Lancet Neurol* **5**, 513-524
8. Davies, J. S., Chung, S. K., Thomas, R. H., Robinson, A., Hammond, C. L., Mullins, J. G., Carta, E., Pearce, B. R., Harvey, K., Harvey, R. J., and Rees, M. I. (2010) The glycinergic system in human startle disease: a genetic screening approach. *Front Mol Neurosci* **3**, 8
9. Chung, S. K., Bode, A., Cushion, T. D., Thomas, R. H., Hunt, C., Wood, S. E., Pickrell, W. O., Drew, C. J., Yamashita, S., Shiang, R., Leiz, S., Longhardt, A. C., Raile, V., Weschke, B., Puri, R. D., Verma, I. C., Harvey, R. J., Ratnasinghe, D. D., Parker, M., Rittey, C., Masri, A., Lingappa, L., Howell, O. W., Vanbellinghen, J. F., Mullins, J. G., Lynch, J. W., and Rees, M. I. (2013) GLRB is the third major gene of effect in hyperekplexia. *Human Mol Genet* **22**, 927-940
10. Chung, S. K., Vanbellinghen, J. F., Mullins, J. G., Robinson, A., Hantke, J., Hammond, C. L., Gilbert, D. F., Freilinger, M., Ryan, M., Kruer, M. C., Masri, A., Gurses, C., Ferrie, C., Harvey, K., Shiang, R., Christodoulou, J., Andermann, F., Andermann, E., Thomas, R. H., Harvey, R. J., Lynch, J. W., and Rees, M. I. (2010) Pathophysiological mechanisms of dominant and recessive GLRA1 mutations in hyperekplexia. *J Neurosci* **30**, 9612-9620
11. James, V. M., Bode, A., Chung, S. K., Gill, J. L., Nielsen, M., Cowan, F. M., Vujic, M., Thomas, R. H., Rees, M. I., Harvey, K., Keramidis, A., Topf, M., Ginjaar, I., Lynch, J. W., and Harvey, R. J. (2013) Novel missense mutations in the glycine receptor beta subunit gene (GLRB) in startle disease. *Neurobiol Dis* **52**, 137-149
12. Butler, A. S., Lindsay, S. A., Dover, T. J., Kennedy, M. D., Patchell, V. B., Levine, B. A., Hope, A. G., and Barnes, N. M. (2009) Importance of the C-terminus of the human 5-HT3A receptor subunit. *Neuropharmacology* **56**, 292-302
13. Chen, X., Webb, T. I., and Lynch, J. W. (2009) The M4 transmembrane segment contributes to agonist efficacy differences between alpha1 and alpha3 glycine receptors. *Mol Membr Biol* **26**, 321-332
14. Harvey, K., Duguid, I. C., Alldred, M. J., Beatty, S. E., Ward, H., Keep, N. H., Lingenfelter, S. E., Pearce, B. R., Lundgren, J., Owen, M. J., Smart, T. G., Luscher, B., Rees, M. I., and Harvey, R. J. (2004) The GDP-GTP exchange factor collybistin: an essential determinant of neuronal gephyrin clustering. *J Neurosci* **24**, 5816-5826
15. Rees, M. I., Harvey, K., Pearce, B. R., Chung, S. K., Duguid, I. C., Thomas, P., Beatty, S., Graham, G. E., Armstrong, L., Shiang, R., Abbott, K. J., Zuberi, S. M., Stephenson, J. B., Owen, M. J., Tijssen, M. A., van den Maagdenberg, A. M., Smart, T. G., Supplisson, S., and Harvey, R. J. (2006) Mutations in the gene encoding GlyT2 (SLC6A5) define a presynaptic component of human startle disease. *Nat Genet* **38**, 801-806
16. Rees, M. I., Harvey, K., Ward, H., White, J. H., Evans, L., Duguid, I. C., Hsu, C. C., Coleman, S. L., Miller, J., Baer, K., Waldvogel, H. J., Gibbon, F., Smart, T. G., Owen, M. J., Harvey, R. J., and Snell, R. G. (2003) Isoform heterogeneity of the human gephyrin gene (GPHN), binding domains to the glycine receptor, and mutation analysis in hyperekplexia. *J Biol Chem* **278**, 24688-24696

17. Thomas, R. H., Chung, S. K., Wood, S. E., Cushion, T. D., Drew, C. J. G., Hammond, C. L., Vanbellinghen, J. F., Mullins, J. G. L., and Rees, M. I. (2013) Genotype-phenotype correlations in hyperekplexia: apnoeas, learning difficulties and speech delay. *Brain In press*
18. Thomas, R. H., Harvey, R. J., and Rees, M. I. (2010) Hyperekplexia: Stiffness, startle and syncope. *J Pediatric Neurol* **8**, 11-14
19. Engel, A. G., Ohno, K., Bouzat, C., Sine, S. M., and Griggs, R. C. (1996) End-plate acetylcholine receptor deficiency due to nonsense mutations in the epsilon subunit. *Ann Neurol* **40**, 810-817
20. Kruger, W., Gilbert, D., Hawthorne, R., Hryciw, D. H., Frings, S., Poronnik, P., and Lynch, J. W. (2005) A yellow fluorescent protein-based assay for high-throughput screening of glycine and GABAA receptor chloride channels. *Neurosci Lett* **380**, 340-345
21. Pless, S. A., Dibas, M. I., Lester, H. A., and Lynch, J. W. (2007) Conformational variability of the glycine receptor M2 domain in response to activation by different agonists. *J Biol Chem* **282**, 36057-36067
22. Hibbs, R. E., and Gouaux, E. (2011) Principles of activation and permeation in an anion-selective Cys-loop receptor. *Nature* **474**, 54-60
23. Grunberg, R., Nilges, M., and Leckner, J. (2007) Biskit--a software platform for structural bioinformatics. *Bioinformatics* **23**, 769-770
24. Wheeler, D. L., Barrett, T., Benson, D. A., Bryant, S. H., Canese, K., Chetvernin, V., Church, D. M., Dicuccio, M., Edgar, R., Federhen, S., Feolo, M., Geer, L. Y., Helmberg, W., Kapustin, Y., Khovayko, O., Landsman, D., Lipman, D. J., Madden, T. L., Maglott, D. R., Miller, V., Ostell, J., Pruitt, K. D., Schuler, G. D., Shumway, M., Sequeira, E., Sherry, S. T., Sirotkin, K., Souvorov, A., Starchenko, G., Tatusov, R. L., Tatusova, T. A., Wagner, L., and Yaschenko, E. (2008) Database resources of the National Center for Biotechnology Information. *Nucleic Acid Res* **36**, D13-21
25. Notredame, C., Higgins, D. G., and Heringa, J. (2000) T-Coffee: A novel method for fast and accurate multiple sequence alignment. *J Mol Biol* **302**, 205-217
26. Eswar, N., John, B., Mirkovic, N., Fiser, A., Ilyin, V. A., Pieper, U., Stuart, A. C., Marti-Renom, M. A., Madhusudhan, M. S., Yerkovich, B., and Sali, A. (2003) Tools for comparative protein structure modeling and analysis. *Nucleic Acid Res* **31**, 3375-3380
27. Pettersen, E. F., Goddard, T. D., Huang, C. C., Couch, G. S., Greenblatt, D. M., Meng, E. C., and Ferrin, T. E. (2004) UCSF Chimera--a visualization system for exploratory research and analysis. *J Comput Chem* **25**, 1605-1612
28. Rees, M. I., Lewis, T. M., Vafa, B., Ferrie, C., Corry, P., Muntoni, F., Jungbluth, H., Stephenson, J. B., Kerr, M., Snell, R. G., Schofield, P. R., and Owen, M. J. (2001) Compound heterozygosity and nonsense mutations in the alpha(1)-subunit of the inhibitory glycine receptor in hyperekplexia. *Hum Genet* **109**, 267-270
29. Brune, W., Weber, R. G., Saul, B., von Knebel Doeberitz, M., Grond-Ginsbach, C., Kellerman, K., Meinck, H. M., and Becker, C. M. (1996) A GLRA1 null mutation in recessive hyperekplexia challenges the functional role of glycine receptors. *Am J Hum Genet* **58**, 989-997
30. Beato, M., Groot-Kormelink, P. J., Colquhoun, D., and Sivilotti, L. G. (2002) Openings of the rat recombinant alpha 1 homomeric glycine receptor as a function of the number of agonist molecules bound. *J Gen Physiol* **119**, 443-466
31. Islam, R., and Lynch, J. W. (2012) Mechanism of action of the insecticides, lindane and fipronil, on glycine receptor chloride channels. *Br J Pharmacol* **165**, 2707-2720
32. Haeger, S., Kuzmin, D., Detro-Dassen, S., Lang, N., Kilb, M., Tsetlin, V., Betz, H., Laube, B., and Schmalzing, G. (2010) An intramembrane aromatic network determines pentameric assembly of Cys-loop receptors. *Nature Struct Mol Biol* **17**, 90-98
33. Kling, C., Koch, M., Saul, B., and Becker, C. M. (1997) The frameshift mutation oscillator (Gla1(sp-d-ot)) produces a complete loss of glycine receptor alpha 1-polypeptide in mouse central nervous system. *Neuroscience* **78**, 411-417
34. Unterer, B., Becker, C. M., and Villmann, C. (2012) The importance of TM3-4 loop subdomains for functional reconstitution of glycine receptors by independent domains. *J Biol Chem* **287**, 39205-39215
35. Villmann, C., Oertel, J., Ma-Hogemeier, Z. L., Hollmann, M., Sprengel, R., Becker, K., Breiting, H. G., and Becker, C. M. (2009) Functional complementation of Gla1(sp-d-ot), a glycine receptor subunit mutant, by independently expressed C-terminal domains. *J Neurosci* **29**, 2440-2452
36. Pless, S. A., and Lynch, J. W. (2008) Illuminating the structure and function of Cys-loop receptors. *Clin Exp Physiol Pharmacol* **35**, 1137-1142

37. Langosch, D., Laube, B., Rundstrom, N., Schmieden, V., Bormann, J., and Betz, H. (1994) Decreased agonist affinity and chloride conductance of mutant glycine receptors associated with human hereditary hyperekplexia. *EMBO J* **13**, 4223-4228
38. Lynch, J. W., Rajendra, S., Pierce, K. D., Handford, C. A., Barry, P. H., and Schofield, P. R. (1997) Identification of intracellular and extracellular domains mediating signal transduction in the inhibitory glycine receptor chloride channel. *EMBO J* **16**, 110-120
39. Rajendra, S., Lynch, J. W., Pierce, K. D., French, C. R., Barry, P. H., and Schofield, P. R. (1994) Startle disease mutations reduce the agonist sensitivity of the human inhibitory glycine receptor. *J Biol Chem* **269**, 18739-18742
40. Saul, B., Kuner, T., Sobetzko, D., Brune, W., Hanefeld, F., Meinck, H. M., and Becker, C. M. (1999) Novel GLRA1 missense mutation (P250T) in dominant hyperekplexia defines an intracellular determinant of glycine receptor channel gating. *J Neurosci* **19**, 869-877
41. Humeny, A., Bonk, T., Becker, K., Jafari-Boroujerdi, M., Stephani, U., Reuter, K., and Becker, C. M. (2002) A novel recessive hyperekplexia allele GLRA1 (S231R): genotyping by MALDI-TOF mass spectrometry and functional characterisation as a determinant of cellular glycine receptor trafficking. *Eur J Hum Genet* **10**, 188-196
42. Rea, R., Tijssen, M. A., Herd, C., Frants, R. R., and Kullmann, D. M. (2002) Functional characterization of compound heterozygosity for GlyRalpha1 mutations in the startle disease hyperekplexia. *Eur J Neurosci* **16**, 186-196
43. Villmann, C., Oertel, J., Melzer, N., and Becker, C. M. (2009) Recessive hyperekplexia mutations of the glycine receptor alpha1 subunit affect cell surface integration and stability. *J Neurochem* **111**, 837-847
44. Estrada-Mondragon, A., Reyes-Ruiz, J. M., Martinez-Torres, A., and Miledi, R. (2010) Structure-function study of the fourth transmembrane segment of the GABArho1 receptor. *Proc Natl Acad Sci USA* **107**, 17780-17784
45. Pons, S., Sallette, J., Bourgeois, J. P., Taly, A., Changeux, J. P., and Devillers-Thiery, A. (2004) Critical role of the C-terminal segment in the maturation and export to the cell surface of the homopentameric alpha 7-5HT3A receptor. *Eur J Neurosci* **20**, 2022-2030
46. Kang, J. Q., Shen, W., Lee, M., Gallagher, M. J., and Macdonald, R. L. (2010) Slow degradation and aggregation in vitro of mutant GABAA receptor gamma2(Q351X) subunits associated with epilepsy. *J Neurosci* **30**, 13895-13905
47. Graham, B. A., Schofield, P. R., Sah, P., Margrie, T. W., and Callister, R. J. (2006) Distinct physiological mechanisms underlie altered glycinergic synaptic transmission in the murine mutants spastic, spasmodic, and oscillator. *J Neurosci* **26**, 4880-4890
48. Ryan, S. G., Buckwalter, M. S., Lynch, J. W., Handford, C. A., Segura, L., Shiang, R., Wasmuth, J. J., Camper, S. A., Schofield, P., and O'Connell, P. (1994) A missense mutation in the gene encoding the alpha 1 subunit of the inhibitory glycine receptor in the spasmodic mouse. *Nat Genet* **7**, 131-135
49. Pless, S. A., Millen, K. S., Hanek, A. P., Lynch, J. W., Lester, H. A., Lummis, S. C., and Dougherty, D. A. (2008) A cation-pi interaction in the binding site of the glycine receptor is mediated by a phenylalanine residue. *J Neurosci* **28**, 10937-10942
50. Wang, Q., and Lynch, J. W. (2011) Activation and desensitization induce distinct conformational changes at the extracellular-transmembrane domain interface of the glycine receptor. *J Biol Chem* **286**, 38814-38824
51. Miraglia Del Giudice, E., Coppola, G., Bellini, G., Ledaal, P., Hertz, J. M., and Pascotto, A. (2003) A novel mutation (R218Q) at the boundary between the N-terminal and the first transmembrane domain of the glycine receptor in a case of sporadic hyperekplexia. *J Med Genet* **40**, e71
52. Bellini, G., Miceli, F., Mangano, S., Miraglia del Giudice, E., Coppola, G., Barbagallo, A., Tagliatela, M., and Pascotto, A. (2007) Hyperekplexia caused by dominant-negative suppression of glyra1 function. *Neurology* **68**, 1947-1949
53. Vergouwe, M. N., Tijssen, M. A., Peters, A. C., Wielaard, R., and Frants, R. R. (1999) Hyperekplexia phenotype due to compound heterozygosity for GLRA1 gene mutations. *Ann Neurol* **46**, 634-638
54. Shiang, R., Ryan, S. G., Zhu, Y. Z., Hahn, A. F., O'Connell, P., and Wasmuth, J. J. (1993) Mutations in the alpha 1 subunit of the inhibitory glycine receptor cause the dominant neurologic disorder, hyperekplexia. *Nat Genet* **5**, 351-358

55. Shiang, R., Ryan, S. G., Zhu, Y. Z., Fielder, T. J., Allen, R. J., Fryer, A., Yamashita, S., O'Connell, P., and Wasmuth, J. J. (1995) Mutational analysis of familial and sporadic hyperekplexia. *Ann Neurol* **38**, 85-91

ACKNOWLEDGEMENTS

JWL is supported by the National Health and Medical Research Council. SKC is supported by an Epilepsy Research UK fellowship. This work was also supported by the Australian Research Council (JWL), Waterloo Foundation (MIR), the National Institute of Social Care and Health Research (NISCHR-RRG; to MIR, RHT and SKC), Wales Gene Park (MIR). We thank Dr Han Lu for help with the voltage-clamp fluorometry experiments.

FIGURE LEGENDS

Fig. 1. Functional characterization of novel mutations using fluorescence-based imaging. A. Normalized glycine EC₅₀ values for receptors comprised of the indicated subunit combinations. Results for p.Q226E and p.V280M containing GlyRs are not shown as complete quench occurred in the absence of glycine. For all other mutated receptors, the absence of a plotted result means that the indicated subunit(s) did not express. B. Mean percentage fluorescence quench observed when NaCl solution was replaced by NaI solution (without glycine). C. Normalized maximal changes in fluorescence observed upon the addition of NaI containing saturating glycine. The maximal change in fluorescence is presented as the final (quenched) fluorescence value minus the initial fluorescence value. D. Mean number of quenched cells expressed as a percentage of the total number of fluorescent cells. In panels A, C and D, all mutant values were normalised relative to the wild type value obtained from the same plate. In all panels, p-values were calculated relative to the α 1 GlyR using one-way ANOVA followed by Dunnett's post-hoc test: * p < 0.05, ** p < 0.01, *** p < 0.001, **** p < 0.0001.

Fig. 2. Functional characterization of autosomal dominant mutations by whole-cell and outside-out patch-clamp recording. A. Sample whole-cell current recording for homomeric p.Q226E GlyRs. In this and all subsequent Figures, horizontal bars indicate the duration of the glycine applications with concentrations shown in μ M. The right panel represents averaged whole-cell glycine dose-response curve for the p.Q226E GlyR. The α 1 GlyR dose-response curve plotted here is replicated in all panels displaying dose-response curves in this and subsequent figures. B. Sample whole-cell current recording and averaged whole-cell glycine dose-response curve for the homomeric p.V280M GlyR. C. Sample whole-cell current recording and averaged whole-cell glycine dose-response curve for the homomeric p.R414H GlyR. Averaged parameters of best fit to all individual dose-response relationships are summarized in Table 2.

Fig. 3. Single channel recordings of homomeric α 1 wild type and spontaneously open mutant GlyRs. A. Single channel current recording of a patch expressing wild type receptors in the absence of glycine. Due to its low open probability in glycine-free solution, the higher resolution recording and accompanying amplitude histogram was obtained in 1 mM glycine. B. A sample recording of spontaneous single channel activity in an outside-out patch expressing p.Q226E, along with the amplitude histogram for the same patch. C. A sample single channel recording from a patch expressing p.V280M receptors, along with the amplitude histogram for the same patch. D. A sample single channel recording from a patch expressing p.R414H receptors, along with the amplitude histogram for the same patch. Channel openings are represented by downward deflections with the mean open current level indicated by dashed lines. The recordings in B-D were made in glycine-free solution. For these recordings, the activity above the horizontal bar in the lower resolution segment is reproduced at higher resolution below. Mean channel conductances and open probabilities are given in the text.

Fig. 4. Functional characterization of autosomal recessive mutations by whole-cell patch-clamp recording and voltage-clamp fluorometry. A. Sample glycine dose-response trace for p.R72C GlyRs co-expressed with the α 1 wild type subunit and normalized glycine dose-response relationship. B. Sample glycine dose-response trace for p.R218W GlyRs co-expressed with the α 1 wild type subunit and normalized glycine dose-response relationship. C. Sample glycine dose-response traces for p.E375X GlyRs expressed together with α 1 wild type or α 1 wild type plus β wild type subunits as indicated. For this and all subsequent current recordings, unfilled bars represent the application of 100 μ M lindane. The lack of lindane inhibition indicates strong expression of β subunits. The α 1 β GlyR dose-response curve plotted here is replicated in all dose-response curve panels in Fig. 5. The bottom panel shows evidence for the efficient incorporation of β subunits into functional GlyRs. α 1 homomeric GlyRs are strongly inhibited by 100 μ M lindane (left), whereas α 1 β GlyRs are resistant (center panel). The right trace, recorded from the same cell as represented

above in panel C, shows that channels formed by the co-expression of p.E375X, $\alpha 1$ and β wild type subunits are also resistant to lindane. Using an unpaired t-test, mean lindane inhibition of these mutated receptors was significantly different to $\alpha 1$ ($p < 0.001$) but not to $\alpha 1\beta$ receptors ($p = 0.393$). D. Normalized glycine dose-response curves for $\alpha 1$ homomeric and $\alpha 1\beta$ heteromeric receptors incorporating p.E375X. Averaged parameters of best fit to all individual dose-response relationships are summarized in Table 2. E. Sample current (black) and fluorescence (grey) responses induced by the application of 10 mM glycine in receptors comprising p.R271C/E375X and $\alpha 1$ wild type subunits and labelled with MTSR. Averaged results are summarized in the text. Control recordings from MTSR-labelled p.R271C GlyRs are also shown.

Fig. 5. Functional characterization of compound heterozygous mutations by whole-cell patch-clamp recording. A. Sample glycine dose-response traces for p.R65W GlyRs expressed together with $\alpha 1$ wild type or $\alpha 1$ wild type plus β wild type subunits as indicated. Normalized glycine dose-response curves for receptors incorporating p.R65W subunits are shown below. B. Sample glycine dose-response traces for p.P230S GlyRs expressed either alone or with the β wild type subunit. Normalized glycine dose-response curves for receptors incorporating p.P230S subunits are shown below. C. Sample glycine dose-response traces for p.L291P GlyRs expressed together with $\alpha 1$ wild type or $\alpha 1$ wild type plus β wild type subunits as indicated. Normalized glycine dose-response curves for receptors incorporating p.L291P are shown below. D. Sample glycine dose-response traces for p.D388A GlyRs expressed together with $\alpha 1$ wild type or $\alpha 1$ wild type plus β wild type subunits as indicated. Normalized glycine dose-response curves for receptors incorporating p.D388A subunits are shown below. Averaged parameters of best fit to all individual dose-response relationships are summarized in Table 2.

Fig. 6. Expression of novel mutations using immunofluorescence. Images for intracellular expression (left) were taken as single cross-sectional confocal images and images for cell surface expression (right) as z-stack images. ++ indicates a high level of cell surface expression comparable with wild type; + indicates a reduction in cell surface expression in comparison to wild type (which was particularly dramatic in the case of p.R65W), and - indicates no visible expression. *R65W with increased master gain.

Fig. 7. Structural modelling of novel mutations. A – F. Major conformational changes compared to wild type receptors are indicated by arrows. TM1 is shown in green, TM2 in blue, TM3 in yellow, TM4 in orange, 0' (R252) in purple and helical extensions in red. G. Pore radius for wild type and three novel autosomal dominant mutations. Arrows indicate the limits of the membrane.

Table 1. Details of hyperekplexia mutations identified in this study.

Case	Genotype	Inheritance mode	Class of mutation	Protein mutation		Protein position	Gender	Reference
1 - 4	Exons 1-7	recessive	deletion	delEX1-7		N-terminal-M2	2x male, 2x female	(29)
5	C573T	compound heterozygote	missense	p.R65W	unknown	N-terminal	male	(10)
	C1068T		missense	p.P230S	unknown	M1		novel
6 - 7	C594T	recessive	missense	p.R72C		N-terminal	2x female	novel
8	C1032T	recessive	missense	p.R218W		N-terminal	male	novel
9	G687A	recessive	missense	p.E103K		N-terminal	male	(10)
10	C971A	recessive	nonsense	p.Y197X		N-terminal	male	(10)
11	C986A	recessive	nonsense	p.Y202X		N-terminal	male	(28)
12	G1033A	compound heterozygote	missense	p.R218Q	paternal	N-terminal	male	(51)
	C1267A		nonsense	p.S296X	maternal	M3		(52)
13	C1056G	dominant	missense	p.Q226E		M1	male	novel
14	G1135A	recessive	missense	p.R252H		M1-M2		(53)
15 - 16	G1192A	dominant	missense	p.R271Q		M2-M3	2x female	(54)
17	A1216G	dominant	missense	p.Y279C		M2-M3	female	(55)
18	G1218A	dominant	missense	p.V280M		M2-M3	male	novel
19	T1252C	compound heterozygote	missense	p.L291P	paternal	M3	female	novel
	A1543C		missense	p.D388A	maternal	M3-M4		novel
20	G1503T	recessive	nonsense	p.E375X		M3-M4	male	novel
21	G1621A	dominant	missense	p.R414H		C-terminal	male	rs200130685*

* p.R414H was a novel variant at the time of identification but since it is listed as a very rare variant in dbSNP.

Table 2. Properties of novel mutations using whole-cell patch-clamp electrophysiology.

	EC₅₀ (μM)	n_H	I_{max} (nA)	n
wild type				
α1	64 \pm 8	3.8 \pm 0.3	19 \pm 3	10
α1β	39 \pm 4	2.4 \pm 0.2	14 \pm 3	5
dominant mutations				
p.Q226E	32 \pm 6	3.5 \pm 0.7	10 \pm 5	3
p.V280M	2.4 \pm 0.3	1.1 \pm 0.2***	5 \pm 4**	3
p.R414H	110 \pm 12	2.3 \pm 0.2*	13 \pm 1	4
recessive mutations				
p.R72C + α1	189 \pm 14	2.9 \pm 0.1	8 \pm 3*	4
p.R218W + α1	235 \pm 26	2.4 \pm 0.2	6 \pm 2**	4
p.E375X + α1	243 \pm 20	1.8 \pm 0.2**	1.2 \pm 0.4*****	4
p.E375X + α1β	140 \pm 22	2.2 \pm 0.2	9 \pm 4	3
compound heterozygous mutations				
p.R65W + α1	1468 \pm 557*****	1.0 \pm 0.1*****	2.9 \pm 1.3*****	6
p.R65W + α1β	1281 \pm 315*****	1.1 \pm 0.2**	1.2 \pm 0.9***	5
p.P230S	172 \pm 50	1.6 \pm 0.1*****	1.6 \pm 0.5*****	6
p.P230S + β	155 \pm 26	2.4 \pm 0.3	2.2 \pm 1.0***	6
p.L291P + α1	198 \pm 15	3.1 \pm 0.5	9 \pm 1*	5
p.L291P + α1β	180 \pm 22	2.2 \pm 0.3	7 \pm 1	4
p.D388A + α1	173 \pm 11	2.8 \pm 0.7	6 \pm 2**	5
p.D388A + α1β	170 \pm 16	2 \pm 0.2	9 \pm 3	4

* p < 0.05, ** p < 0.01, *** p < 0.001, ***** p < 0.0001 relative to the corresponding homo- or heteromeric wild type GlyR via one-way ANOVA followed by Dunnett's post-hoc test.

Figure 1

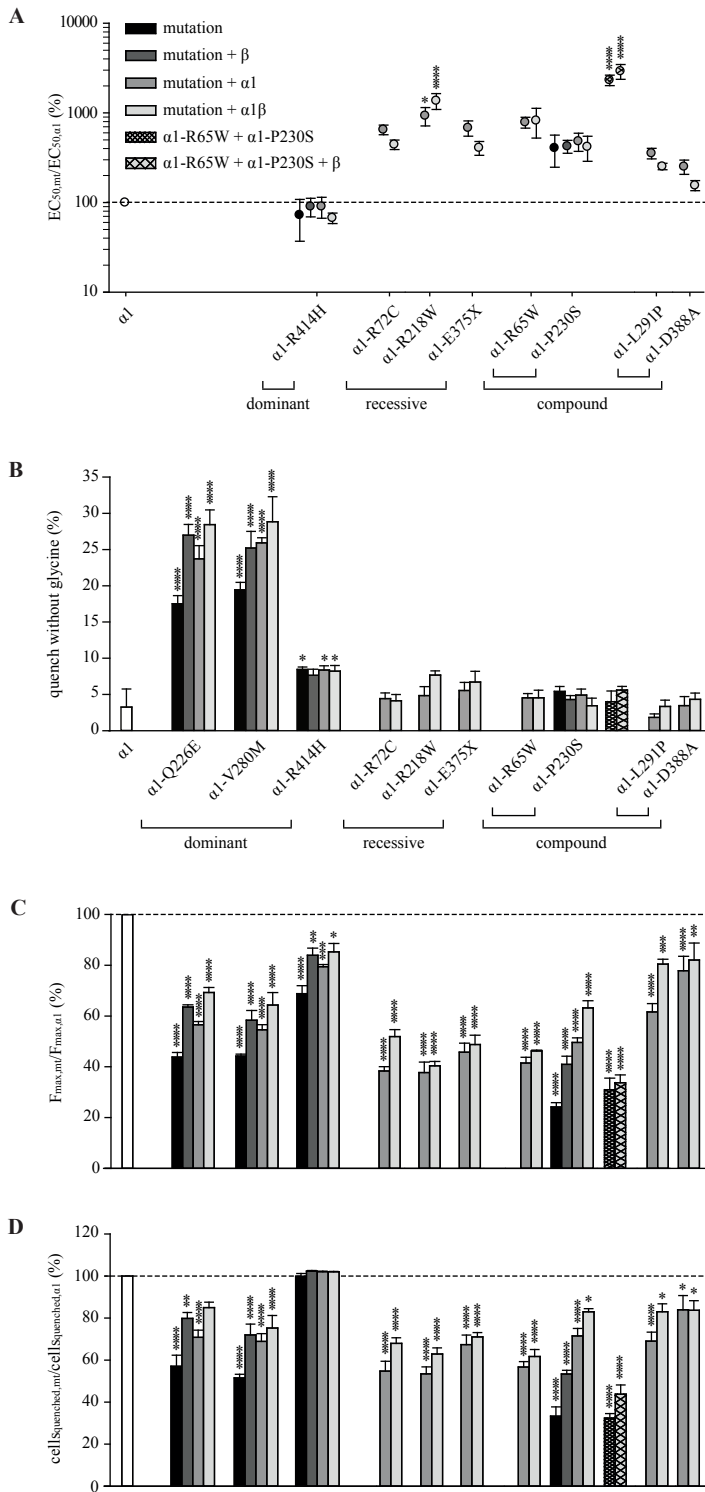


Figure 2

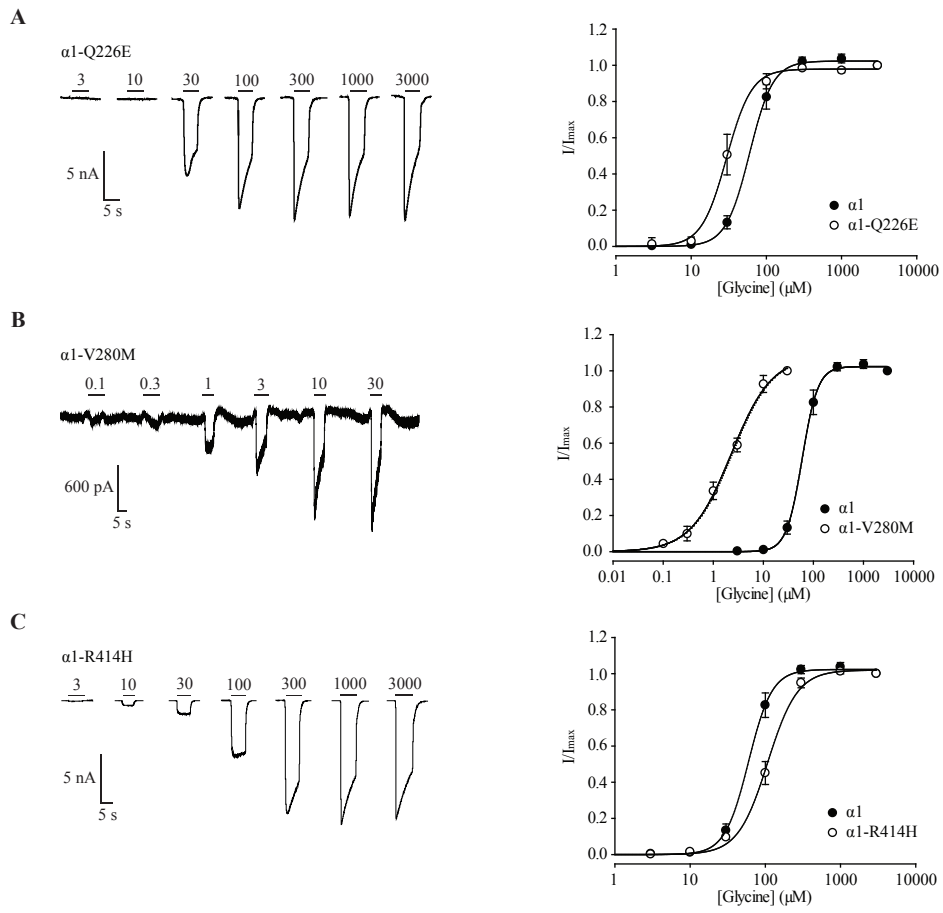


Figure 3

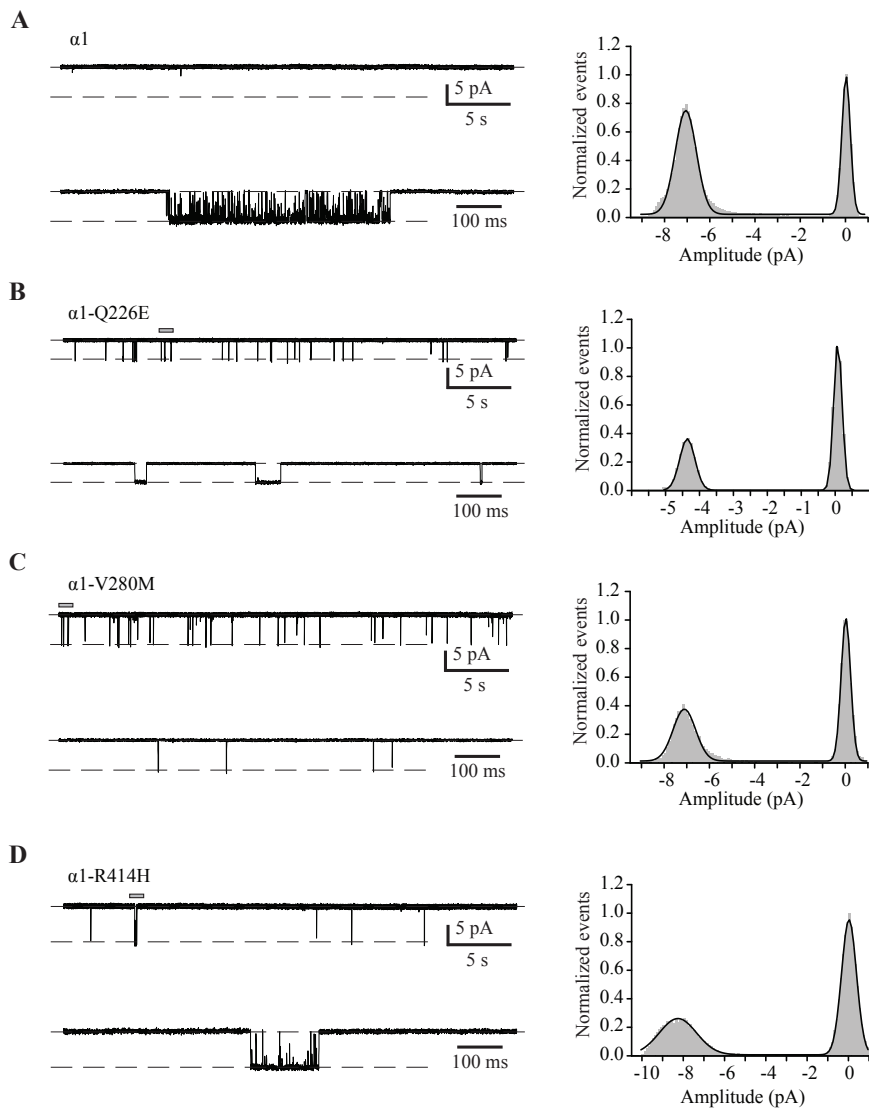


Figure 4

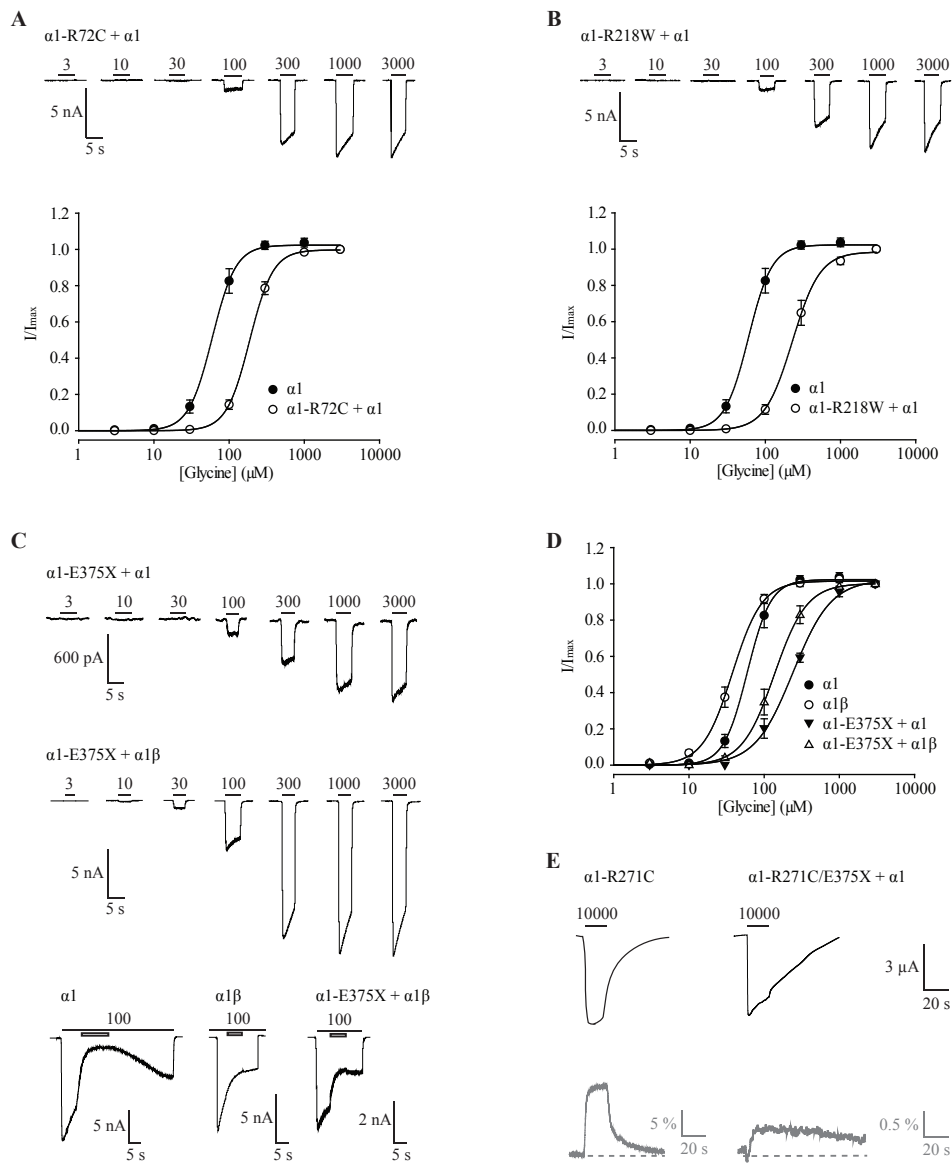


Figure 5

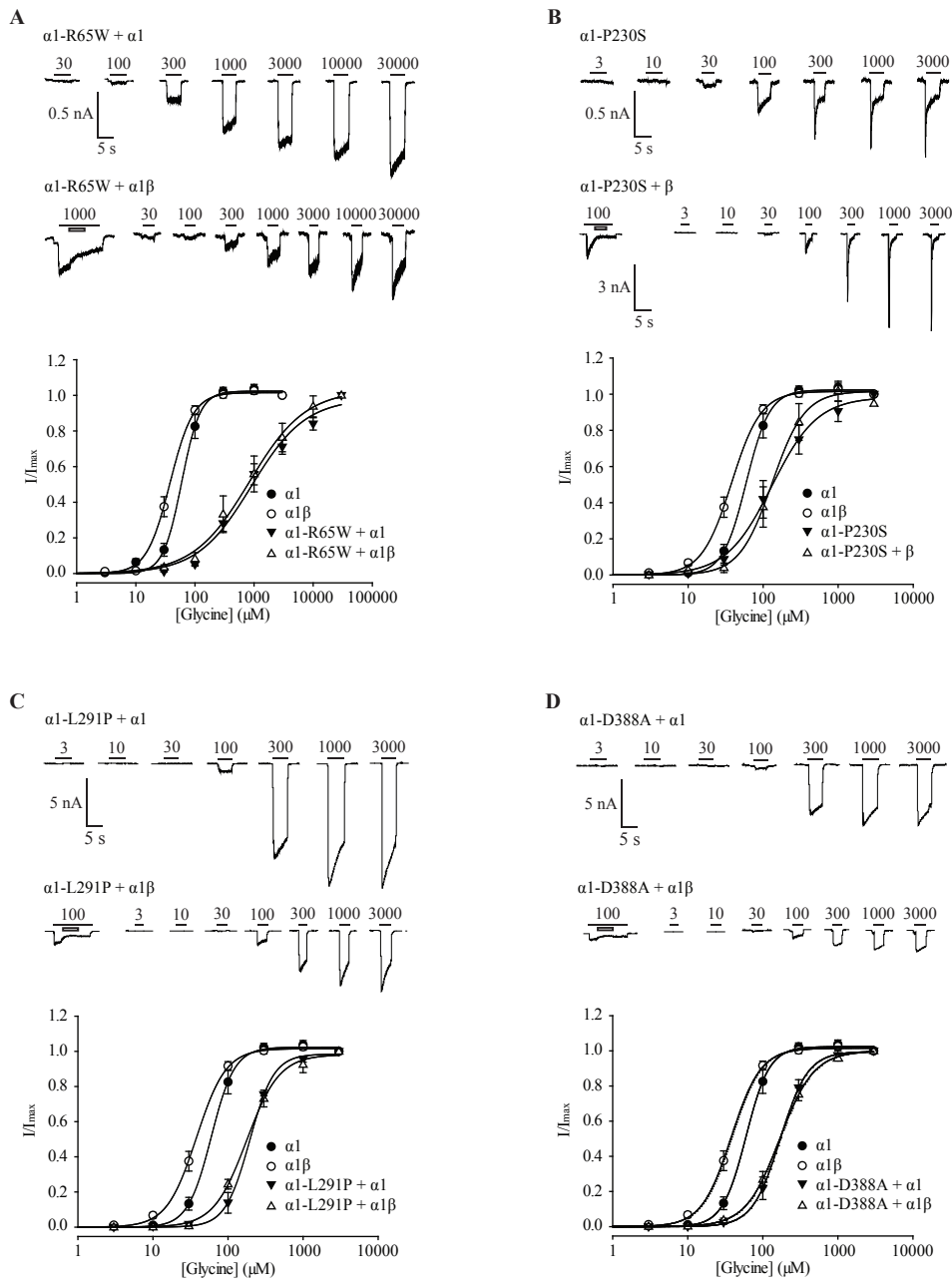


Figure 6

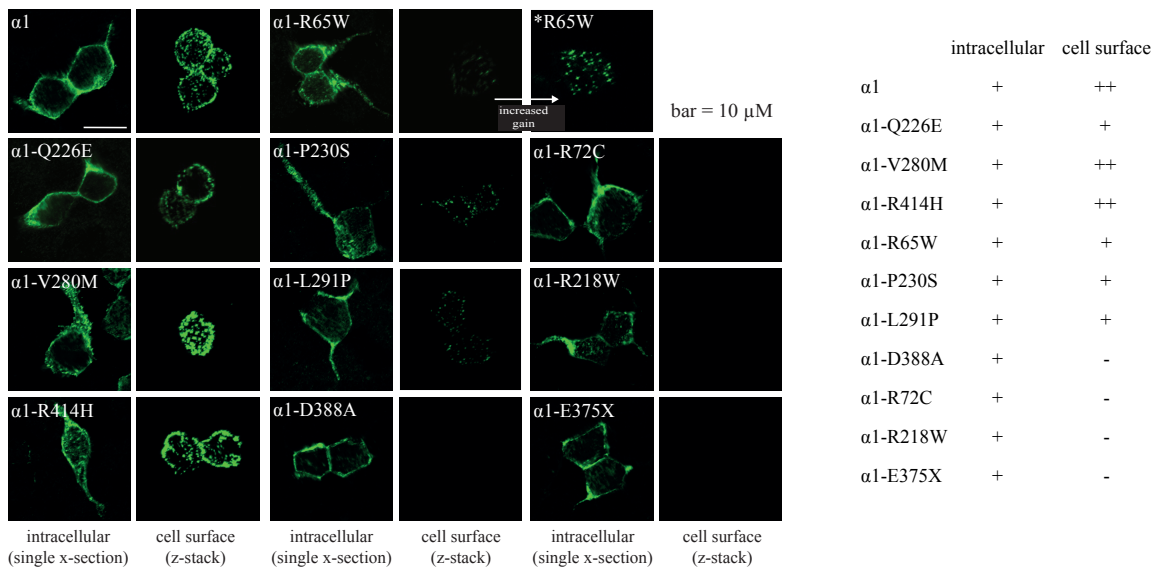


Figure 7

